Anisotropic paramagnetic susceptibility of crystalline ruby at cryogenic temperatures

John G. Hartnett*, Jean-Michel Le Floch*†, Michael E. Tobar* Jerzy Krupka‡, Pierre-Yves Bourgeois§,
*School of Physics, the University of Western Australia, 35 Stirling Hwy, Crawley 6009 WA Australia
Email: john@physics.uwa.edu.au
†Xlim, UMR CNRS 6172, 123, av. Albert Thomas 87060 Limoges Cedex, France
‡Institute of Microelectronics and Optoelectronics, Department of Electronics,
Warsaw University of Technology, Warsaw, Poland
§FEMTO-ST, CNRS 32 av. de l'Observatoire, 25044 Besançon, France

***Abstract*—The static paramagnetic susceptibility of chromium ions in sapphire (Cr^{3+} in Al_2O_3) in zero applied static magnetic field has been determined between 4.2 K and 100 K using the Whispering Gallery mode technique at microwave frequencies. Although sapphire exhibits a uniaxial anisotropy in permittivity, in contrast the magnetic susceptibility has been measured to only have a susceptibility component perpendicular to the crystal axis. This component showed a strong Curie law dependence below 30 K.**

I. Introduction

The whispering gallery (WG) mode method has proved to be a very accurate method for measurements of the complex permittivity of extremely low-loss dielectrics. The method has been employed for very precise measurements of the permittivity and the dielectric losses of both isotropic and uniaxial anisotropic materials. [1], [8], [9] Very low-loss single-crystal materials including sapphire, Titanium doped sapphire, YAG, Chromium doped YAG, Calcium, Magnesium and Barium Fluoride, quartz, and others have been measured this way. [2]–[4], [7], [10], [18]

In this research, the electrical and magnetic properties of a cylinder of single crystal ruby were analyzed between 4.2 K and room temperature and at microwave frequencies between 8 and 18 GHz. The analysis is presented in terms of the anisotropic loss tangent of ruby and the temperature and frequency dependence of the anisotropic components of the real (dispersive) and imaginary (lossy) parts of the magnetic susceptibility resulting from the inclusion of paramagnetic Cr^{3+} ions in the sapphire lattice (Al_2O_3).

The chromium (Cr^{3+}) ion concentration was estimated by the manufacturer to be about 3% by weight, giving the crystal a ruby red colour. Cr^{3+} ions in this sample will be treated as a dilute spin system within the sapphire lattice.

Sapphire has a predominantly hexagonal crystal structure with a slight trigonal distortion. Previous research has shown it to have anisotropic components of both loss tangent and permittivity. [6], [17] The Cr^{3+} ions in the lattice will both contribute therefore to a small paramagnetic susceptibility as well as modify the loss tangent and permittivity of the sapphire. Previously the real part of the paramagnetic susceptibility was measured in a nominally pure sapphire sample at a fixed temperature of 4.2 K. [12], [19] In this work we present the analysis over a range of temperatures from 4.2 K to 100 K.

II. Measurement Technique

The most effective way to eliminate cavity conductor losses as well as radiation losses in accurate dielectric permittivity and loss tangent measurements is to use high-order Whispering Gallery (WG) modes in cylindrical specimens of the material under test. In order to evaluate the permittivity tensor components of a uniaxial anisotropic material, a cylindrical specimen is made with its crystal axis aligned to the cylinder axis. Then two WG modes are chosen that exhibit quasi-TE and quasi-TM field structures. Finally, a system of two nonlinear determinant equations is solved to evaluate permittivity tensor components. From permittivity components, resonance frequencies for several other modes are computed and compared with experiment, to check the validity of the mode identification. For a more thorough explanation of the method refer to references [1], [8], [9].

Once permittivity components are found, loss tangents are evaluated as solutions to the equations,

$$Q_i^{-1} = p^i_{\epsilon\perp} tan\delta_\perp + p^i_{\epsilon||} tan\delta_{||} + p^i_{m\perp}\chi''_\perp + p^i_{m||}\chi''_{||} + L_{rad}. \quad (1)$$

where $i = WGE$ or WGH represents either type of WG mode; $tan\delta_\perp$ and $tan\delta_{||}$ are the dielectric loss tangents of the crystal perpendicular and parallel to the anisotropy axis; $p^i_{\epsilon\perp}$ and $p^i_{\epsilon||}$ are the electric energy filling factors perpendicular and parallel to the anisotropy axis, and $p^i_{m\perp}$ and $p^i_{m||}$ are the respective magnetic energy filling factors. The parameters $\chi''_\perp$ and $\chi''_{||}$ represent the imaginary part of the magnetic susceptibility resulting from the paramagnetic ions and describe the magnetic losses introduced by the doping process and L_{rad} represents the radiation losses. Equation (1) assumes that only one paramagnetic species is present.

A cylindrical ruby crystal was mounted at the center of a copper cavity of internal length 43.0 mm and internal diameter 60.5 mm but the cylindrical shield was removed and replaced with four support posts on the same circumference. The crystal

1-4244-0647-1/07/$20.00 ©2007 IEEE

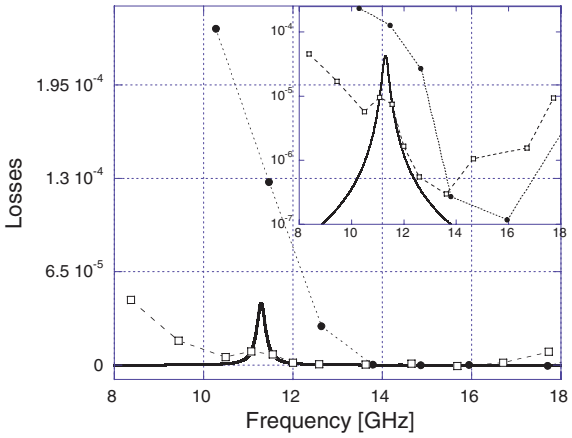

Fig. 1. Magnetic and radiation losses (Q_*^{-1}) of resonant modes as a function of frequency at room temperature (see eq. (5)). The open squares are data from the WGH modes and the solid circles are from the WGE modes. The same data is also shown on a vertical log plot to more clearly see the fit. The solid line is the curve fit of (2). The broken lines are guides for the eye.

was supported in the cavity by a central support post. The cavity was placed in a vacuum enclosure lined with microwave absorber. This means at low frequencies the main microwave losses are due to radiation. At high frequencies radiation losses may be neglected entirely as having negligible effect on the measured Q-factor, hence $L_{rad} \rightarrow 0$ in (1).

The ruby cylinder has a diameter of 29.97 $\pm$ 0.005 mm and a length of 23.86 $\pm$ 0.005 mm. The cavity was fitted with two coupling loops positioned at two opposite sides of the symmetry plane of the cavity. The loops were rotated either 0^o or 90^o with respect to the plane of symmetry, to couple to either the WGE or to the WGH modes. At room temperature, the coupling loops were adjusted to obtain very weak coupling to higher order azimuthal modes, that is with azimuthal mode numbers greater than 7. With decreasing temperature, the coupling coefficients remained reasonably small and with each measurement the mode frequency, coupling and unloaded Q-factor was measured using a Q-circle fit technique.

The resonator was coupled to a vector network analyzer in reflection. The polar magnitude of the reflection coefficient was stored on a computer and then software was used to extract values of coupling, frequency and unloaded Q-factor from the best fit data. Measurements were made at room temperature (300 K) and then at 77 K. The vacuum enclosure was evacuated and cooled to 77 K with liquid nitrogen, and then to 4.2 K with liquid helium. The computer controlled an automatic program to sample the resonance frequencies as a function of temperature, collecting data for a few modes at a time from 4.2 K to about 120 K.

Initially the resonance frequencies and Q-factors of the modes of the two orthogonal types, WGE and WGH modes, were determined at 300 K and at 77 K and are shown in Table I. The modes have been labeled N(S)X-m according to Krupka [10] where N or S respectively indicate whether the magnetic field is anti-symmetric or symmetric with respect to the plane of the coupling loops. The parameter X indicates the order of increasing value of the frequency within a mode family and m is the azimuthal mode number. The mode type is clearly identified by its electric and magnetic energy filling factors. The values of both electric and magnetic filling factors were calculated once the relative permittivity was known. For WG modes they are close to 1 or 0, and of opposite value for pure WGE or WGH modes. See Table I. They represents a particular dominant polarization either perpendicular or parallel to the crystal axis.

III. Paramagnetism

The chromium (Cr^{3+}) ion introduces a well described electron spin resonance (ESR) into ruby that has been exploited as a ruby maser. Paramagnetism usually results in an ion where unpaired electrons exist in an outer orbital shell. In a crystalline solid, paramagnetic ions contribute to a net magnetic susceptibility as a result of an external magnetic field, which may be from the applied microwave signal used to interrogate the resonance in a dielectric resonator. At constant temperature, the complex ac magnetic susceptibility ($\chi = \chi' - j\chi''$) may be described as a function of frequency with a Lorentzian line shape [13], [14] where no inhomogeneous line broadening mechanisms are in place. In this case the real part may be written

$$\chi_i' = \chi_0^i 2 f_L^2 \frac{f^2 - f_L^2}{(f^2 - f_L^2)^2 + f^2 \Delta f_L^2}, \tag{2}$$

and the imaginary part as

$$\chi_i'' = \chi_0^i 2 f_L^2 \frac{f \Delta f_L}{(f^2 - f_L^2)^2 + f^2 \Delta f_L^2}, \tag{3}$$

where $i = \perp$ or $||$ for the isotropy axes. Δf_L is the full width at half maximum (FWHM) of the Lorentzian curve, χ_0^i the static or dc magnetic susceptibility, and f_L is the ESR line frequency.

In zero applied dc magnetic field the lowest frequency ESR line occurs in ruby at $f_L = 11.456$ GHz. [16] Far above the spin resonance frequency where $f \gg f_L$ the losses are dominated by the dielectric losses in the crystal. See column 3 of Table I. Q-factor rises to a maximum as a function of frequency then starts to decrease. Therefore between 13 GHz and 18 GHz in both mode families at room temperature Q^{-1} should result from the dielectric losses only. At these frequencies the radiation losses can be neglected. In the WG modes studied, one electric filling factor is approximately zero, therefore we can also easily neglect that term and solve (1) for the loss tangent, $tan\delta_\perp$ or $tan\delta_{||}$, at the specified frequencies of the available data.

We solved (1) for $tan\delta_{||}$ from the WGH modes with $f > 13$ GHz, while ignoring $\chi_\perp''$, $\chi_{||}''$ and L_{rad}. After taking a power law fit through the results we got,

$$tan\delta_{||} = 4.56 \times 10^{-7} f^{0.86}. \tag{4}$$

It was expected that $tan\delta$ should have a frequency dependence of order f^x where $x = 1$. This is indicated in (4) as $x \approx 1$.

TABLE I
WHISPERING GALLERY MODE DATA

	m	$f(300K)$	$Q(300K)$	$f(77K)$	$Q(77K)$	$p_{\epsilon\perp}$	$p_{\epsilon\|\|}$	$p_{m\perp}$	$p_{m\|\|}$	*Label*
WGH modes										
	6	8.3758	2.05 10^4	8.4622		0.0761	0.9023	0.8199	0.0117	N1-6
	7	9.4405	4.86 10^4	9.5394	2.86 10^4	0.0589	0.9221	0.8348	0.0091	N1-7
	8	10.4972	1.06 10^5	10.6076		0.0464	0.9356	0.8474	0.0070	N1-8
	9	11.5468	8.80 10^4			0.0391	0.9468	0.8581	0.0057	N1-9
	10	12.5873	2.15 10^5	12.7187		0.0323	0.9546	0.8674	0.0046	N1-10
	11	13.6233	2.13 10^5	13.7699	9.40 10^5	0.0275	0.9620	0.8751	0.0038	N1-11
	12	14.6552	1.76 10^5	14.8133	9.69 10^5	0.0241	0.9665	0.8817	0.0031	N1-12
	13	15.6830	2.36 10^5	15.8524	1.07 10^6	0.0207	0.9701	0.8878	0.0026	N1-13
	14	16.7064	1.50 10^5	16.8872	1.72 10^6	0.0182	0.9730	0.8933	0.0022	N1-14
	15	17.7267	6.80 10^4	**17.9191**	2.64 10^6	0.0152	0.9759	0.8983	0.0019	N1-15
	7	11.0689	6.43 10^4			0.3785	0.5948	0.8150	0.0855	N2-7
	8	11.9984	1.36 10^5	12.1132		0.3184	0.6586	0.8363	0.0611	N2-8
WGE modes										
	6	10.2819	4.1 10^3			0.9204	0.0197	0.0502	0.9191	S2-6
	7	11.4684	7.3 10^3	11.5485	1.14 10^4	0.9356	0.0143	0.0415	0.9356	S2-7
	8	12.6433	2.76 10^4	12.7345	2.60 10^4	0.9447	0.0153	0.0391	0.9426	S2-8
	9	13.7960	1.07 10^5	13.9025	2.96 10^5	0.9380	0.0271	0.0577	0.9345	S2-9
	9	14.8668	1.22 10^5	14.9847	3.22 10^5	0.8359	0.1366	0.2730	0.7071	S4-9
	10	15.9448	1.18 10^5	16.0658	4.14 10^5	0.8624	0.1120	0.2319	0.7539	S4-10
	11	17.0292		17.1575	2.23 10^5	0.8786	0.0963	0.2028	0.7854	S4-11
	12	18.0913	9.0 10^4	18.2525	1.28 10^6	0.8903	0.0859	0.1822	0.8081	S4-12
	12	17.7110	1.3 10^5	**17.7130**	2.69 10^6	0.9296	0.0451	0.1023	0.8923	N3-12

Col (1): m is the azimuthal mode number. Cols (2) and (4): units in GHz. Cols (6) and (7) are the electric filling factors, Cols (8) and (9) are the magnetic filling factors computed numerically. Col (10): modes labeled N(S)X-m with N or S for anti-symmetric and symmetric magnetic fields, X is the order of increasing frequency and m is the azimuthal mode number.

Using (4) to subtract $tan\delta_{||}$ from Q^{-1} with the appropriate electric energy filling factors the microwave losses

$$Q_*^{-1} = p^i_{m\perp}\chi''_\perp + p^i_{m||}\chi''_{||} + L_{rad}, \tag{5}$$

were determined for each WGH mode, particularly at lower frequencies where these losses are significant. The results are shown in fig. 1 from 8 GHz to 18 GHz at 300 K. The procedure was repeated for the WGE modes but because radiation losses dominate at low frequency they would erase any spin resonance peak if it was present. Far above the spin resonance (i.e. $f \gg f_L$), the magnetic and radiation losses are approximately zero.

From the best fit of (2) to the available data it was determined that $\Delta f_L = 0.24 \pm 0.06$ GHz, $f_L = 11.29 \pm 0.19$ GHz and $\chi_0^\perp = (5.38 \pm 0.80) \times 10^{-7}$ at room temperature. The line frequency is slightly shifted from that measured at 4.2 K. [16] More data is needed for a better resolution of the line but it was not possible to find any more WG modes in the sample with a frequency close to the spin resonance.

The same measurements were repeated at 77 K, however the losses around 11.6 GHz were much greater and no resonant mode could be found in that region of the spectrum, nor could the Q-factors be reliably measured for modes either side. As a result they are not listed in Table I.

IV. TEMPERATURE DEPENDENCE

For absolute temperatures sufficiently low enough (at least where $T < 30\ K$) the fractional frequency temperature dependence of a resonance mode in crystalline sapphire with only one paramagnetic species can be correctly represented by [11]

$$\frac{f_0 - f}{f_0} = AT^4 - C(T), \tag{6}$$

where f_0 is the expected frequency of the mode at absolute zero with no paramagnetic ions present. The value of A depends on the mode type and the electric-energy filling factor. The exponent of the frequency-temperature power law was found from data fits to the pure (non deliberately doped) sapphire. It is consistent with the low temperature thermal expansion of sapphire. [5] The second term of (6) is the paramagnetic or Curie term ($C(T)$) resulting from the ac magnetic susceptibility:

$$C(T) = \frac{1}{2}p^i_{m\perp}\chi'_\perp + \frac{1}{2}p^i_{m||}\chi'_{||}, \tag{7}$$

where the magnetic-energy filling factors ($p^i_{m\perp}$, $p^i_{m||}$) determine the anisotropic components of the real susceptibility. In turn, in a weak applied magnetic field these paramagnetic components are described using (2) and van Vleck's equation for a three-energy-level system for the dc magnetic susceptibility, [15]

$$\chi_0^i = N\left[\frac{a}{T}\sum_{n=0}^{2}(g_i^n)^2 exp(-\delta_n/k_BT) + \sum_{n=0}^{2}\alpha_i^n exp(-\delta_n/k_BT)\right]\Gamma^{-1} \tag{8}$$

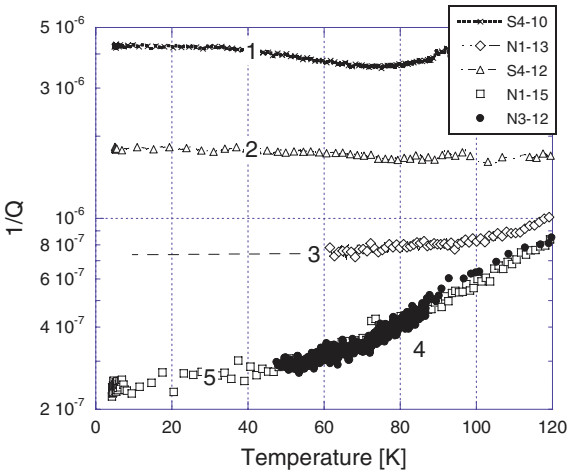

Fig. 2. Q^{-1} for the modes of increasing frequency: S4-10 (curve 1), S4-12 (curve 2), N1-13 (curve 3), N3-12 (curve 4) overlays some of N1-15 (curve 5). Only 5% of the actual data are shown for clarity. The lower temperature Q-factor data for curves 3 and 4 was poorly resolved and is therefore not used.

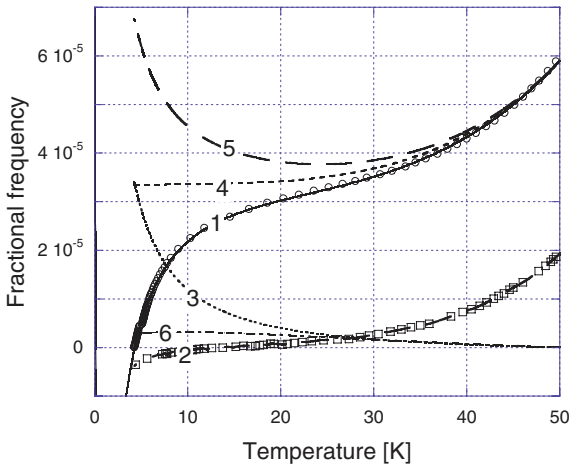

Fig. 3. Fractional frequency data with curve fits of the N1-15 mode (curve 1) and the N3-12 mode (curve 2) between 4.2 and 50 K. For clarity only 10% of the actual data points are displayed. Curve 3 represents the Curie term $C(T)$ and curve 4 the lattice term AT^4 of eq. (6). Curve 5 is the sum of curve 3 and 4. The quality of the curve fits is quantified by the statistical χ^2 parameter (not to be confused with χ used elsewhere in this paper), which for curve 1, $\chi^2 = 4.42 \times 10^{-11}$ and for curve 2, $\chi^2 = 1.56 \times 10^{-11}$. Curve 6 shows the contribution to the susceptibility of the N1-15 mode from the small van Vleck ($\alpha^n_\perp$) coefficients.

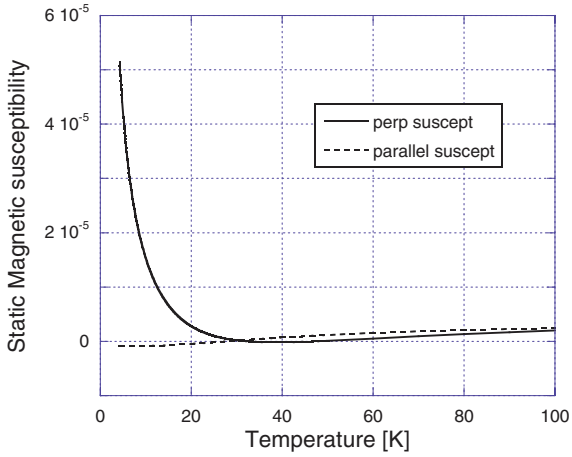

Fig. 4. Static paramagnetic susceptibility perpendicular (curve 1) and parallel to the crystal axis (curve 2) between 4.2 and 100 K.

where $i = \perp$ or $||$ represents the anisotropy axes, N is the paramagnetic ion concentration, g_i^n is the Landé factor and $\delta_n = E_n - E_0$ is the energy difference, where E_n $(n > 0)$ represents the energy of an excited state and E_0 the energy of the ground state. The normalizing term is given by

$$\Gamma = \sum_{n=0}^{2} exp(-\delta_n / k_B T). \tag{9}$$

The parameter $a = \mu_B^2 J(J+1)/3k_B$ where μ_B the Bohr magneton, k_B Boltzmann's constant and J is the equivalent total angular momentum of the ground state ion.

When the temperature of the spin system is such that $k_B T \gg ZFS$, the Zero Field Splitting energy, which results in the crystal field due to the inclusion of the impurity ion, it is expected that the magnetic susceptibility will follow a simple Curie law $1/T$ dependence. For Cr^{3+} ions in sapphire the ratio $ZFS/k_B = 0.56$ K but where an additional excited state exists at higher equivalent temperatures and is expected to be thermally excited, (8) is necessary for a full description.

The mode frequency and the loaded Q-factor of five WG modes was recorded continuously over a period of days as the crystal was warmed slowly in the cryostat. The loss data (1/Q) are shown in fig. 2. From this it is apparent that except for the two modes near 18 GHz the others are dominated by radiation and/or magnetic losses. Only where the mode frequency is sufficiently high enough are radiation losses negligible and the magnetic losses small. This is where the microwave losses are primarily limited by the dielectric loss tangent. The two highest Q-factor modes, that were accessible with available equipment, N1-15 (WGH at 17.923 GHz) and N3-12 (WGE at 17.715 GHz), were thus chosen for further analysis. These have been highlighted in bold print in Table I.

As the temperature tends to absolute zero the right hand term of (8) tends to a constant and by algebraic rearrangement may be written as

$$N\alpha_i^0 + \left[-N(\alpha_i^0 - \alpha_i^1)exp(-\delta_1/k_BT) \right. \\ \left. -N(\alpha_i^0 - \alpha_i^2)exp(-\delta_2/k_BT)\right]\Gamma^{-1}. \tag{10}$$

Therefore, from the frequency data, χ_0^i can only be resolved to within an unknown constant $(N\alpha_i^0)$. This introduces an arbitrary offset that involves the precise value of f_0 and therefore introduces the biggest error into determining the smaller van Vleck coefficients (α_i^n). However their differences can be determined very precisely.

Using (10) in (8) and after combining with (6) and (7), the result was applied to the data for temperatures less than 50 K using a least squares fitting algorithm. We assumed a value

TABLE II
VAN VLECK CURVE FIT PARAMETERS

	g_i^0	g_i^1	g_i^2	$N(\alpha_i^0 - \alpha_i^1)$	$N(\alpha_i^0 - \alpha_i^2)$	Na
$i = \perp$	1.75 ± 0.25	2.20 ± 0.25	0	$(2.39 \pm 0.02) \times 10^{-5}$	$(-4.21 \pm 0.09) \times 10^{-5}$	$(6.86 \pm 0.07) \times 10^{-5}$
$i = \|\|$	-	-	0	$(1.82 \pm 0.04) \times 10^{-6}$	$(-1.49 \pm 0.05) \times 10^{-5}$	-

of $\Delta f_L = 0.1$ GHz as it could not be determined from the data. At room temperature it was measured to be about 0.24 GHz. We also know that it must be larger near 77 K because no resonance was found near 11.45 GHz. However it was measured in nearly pure sapphire with $\Delta f_L = 9$ MHz. [19] Also in YAG the chromium line width decreased on cooling from 100 K (see ref. [3]) therefore 0.1 GHz was assumed as a reasonable estimate here. This means the temperature independent part of χ_i' in (2) can be assumed constant over the temperature range of interest because $f - f_L \gg \Delta f_L$.

The best fit lattice parameters for f_0 and A from (6) were estimated from the fractional frequency data for the two modes shown in fig. 3. For the N1-15 WGH mode $A = (4.51 \pm 0.05) \times 10^{-12}$ and for the N3-12 WGE mode $A = (3.192 \pm 0.006) \times 10^{-12}$. The ratio of these values 0.71 is indicative of the anisotropy in the dielectric permittivity perpendicular and parallel to the ruby crystal axis.

The Curie law term was initially evaluated from the low temperature N1-15 data (curve 1 in fig. 3), which allowed the evaluation of the parameter Na in (8). That is, $g_\perp^2$ and $\alpha_\perp^n$ were set to zero and a fit to the N1-15 data for temperatures less than 20 K was initially performed. Then using the resulting value of Na a fit was carried out to the data up to 50 K. The following resulted. The best fit g-factors $g_\perp^0 = 1.75 \pm 0.25$ and $g_\perp^1 = 2.20 \pm 0.25$ are consistent with the published value of 1.98 for the ground state. [16] The parameter $g_\perp^2$ was found to be consistent with zero. Because the excited energy level (δ_2 above the ground state) is so far above the energies associated with the applied microwave field it cannot be directly excited by microwave photons. Only the much weaker van Vleck (α) coefficients quantify some sort of quantum mechanical mixing of this state into the ground state. The ZFS of the ground state (with energy δ_1) is populated directly by the microwave photons in resonance with the spin system, while the excited state is only thermally populated.

The ZFS energy of the ground state equivalent to $\delta_1/k_B = 0.56$ K (or 11.45 GHz), could not be determined from the fits, so this value was assumed. However a best fit parameter consistent with an unidentified excited energy level yielded $\delta_2/k_B = 58.47 \pm 1.49$ K. Could this be the result of spin exchange of interacting pairs, because the concentration of 3% chromium ions may be higher than allowable for a dilute non-interacting system?

The fits to N3-12 data (curve 2 in fig. 3) were not sensitive to any values of $g_{||}^n$, and hence they were set to zero. This means there was no detectable Curie law dependence in the parallel component of the static magnetic susceptibility ($\chi_0^{||}$). In fact, the Curie law term (Na/T) seen in curve 2 can be accounted for almost entirely by the perpendicular susceptibility and the much smaller perpendicular magnetic filling factor in the N3-12 mode. Only the much smaller van Vleck ($\alpha_{||}^n$) coefficients were used to obtain a fit to the small residuals. The best fit van Vleck parameters obtained from the analysis are shown in Table II. Dashes are used where no data were obtainable. Curve 6 of fig. 3) shows the contribution to the susceptibility of the N1-15 mode from the small van Vleck ($\alpha_\perp^n$) coefficients.

Since both of the 18 GHz modes analyzed here have frequencies greater than the spin resonance frequency (f_L) the sign of the ac susceptibility from (2) is positive, therefore the Curie term (curve 3 in fig. 3) does not produce a frequency temperature turnover point when added to the lattice term (curve 4 in fig. 3). If the resonance frequency had been below the ESR frequency the sign of the ac susceptibility from (2) would instead have been negative and it would have produced a turnover point as illustrated by curve 5 in fig. 3.

From the curve fitting analysis it was found that the resultant static magnetic susceptibility components, shown in fig. 4, represent a significant $\chi_0^\perp$ component (curve 1) but only an upper limit on the $\chi_0^{||}$ component (curve 2). By taking the ratio of these two curves below 20 K, after normalizing for the $1/T$ Curie law dependence, an effective angle of misalignment of the crystal axis from the cylinder axis may calculated. The residual parallel magnetic susceptibility was found to be consistent with an axis misalignment $\leq 0.5^o$. This means that the measured parallel magnetic susceptibility component (the broken curve in fig. 4) represents an upper limit only.

The static magnetic susceptibility perpendicular to the isotropy axis was determined previously [19] to be $\chi_0^\perp = 5.9 \times 10^{-8}$ at 4.2 K in a nominally pure sapphire, where a residual concentration of chromium ions was leftover from the manufacturing process. In that sample N was estimated to be only a few parts per million (ppm). However by comparing $\chi^\perp$ of the latter to our result here, at 4.2 K, $\chi_0^\perp = 5.24 \times 10^{-5}$ in ruby with a 3% by weight concentration of Cr^{3+} ions means the nominally pure sapphire, in fact, has a concentration of about $3.4 \times 10^{-3}\%$ by weight or about 34 ppm of Cr^{3+} ions. The nominally pure sapphire did have a pinkish tinge and so such a concentration is consistent with this.

V. CONCLUSION

The dc or static paramagnetic susceptibility has been determined for a ruby crystal with approximately 3% by weight of chromium ions. It was shown to have classic Curie law behaviour below 30 K. However only the component of the magnetic susceptibility perpendicular to the crystal isotropy axis was significant. Within tolerances of the machining of the crystal the small measured residuals seen for the parallel component of the magnetic susceptibility

may in fact be due misalignment of the cystal axis with the cylinder axis.

ACKNOWLEDGMENT

This work was supported by the Australian Research Council.

REFERENCES

[1] J. Baker-Jarvis, R. G. Geyer, J. H. G. Jr, M. D. Janecic, C. A. Jones, B. Riddle, C. M. Well, and J. Krupka, "Dielectric charaterization of low-loss materials," *IEEE Trans. Dielectric Electric. Insul.*, vol. 5, pages 571-577, 1998.

[2] J. G. Hartnett, M. E. Tobar, and J. Krupka, "Complex paramagnetic susceptibility of titanium doped sapphire," *J. Phys. D: Appl. Phys.*, vol. 34, pages 959-967, 2001.

[3] J. G. Hartnett, A. N. Luiten, J. Krupka, M. E. Tobar, and P. Bilski, "Influence of paramagnetic chromium ions in crystalline YAG at microwave frequencies," *J. Phys. D: Appl. Phys.*, vol. 35, pages 1459-1466, 2002.

[4] J. G. Hartnett, A. C. Fowler, M. E. Tobar, and J. Krupka, "The microwave characterization of single crystal Lithium and Calcium Fluoride at cryogenic temperatures," *Trans on UFFC*, vol. 51, pages 380-385, 2004.

[5] J.G. Hartnett, M.E. Tobar, J. Krupka, "The dependence of the permittivity of sapphire to thermal deformation at cryogenic temperatures," *Meas. Sci. Tech.* vol. 15, pages 203 - 210, 2004.

[6] J.G. Hartnett, M.E. Tobar, E.N. Ivanov and J. Krupka, "Room temperature measurement of the anisotropic loss tangent of sapphire using the whispering-gallery-mode technique," *IEEE Trans. on UFFC*, vol. 53, pages 34-38, 2006

[7] M. V. Jacob, J. G. Hartnett, J. Mazierska, J. Krupka, and M. E. Tobar, "Dielectric Characterisation of Barium Fluoride at Cryogenic Temperatures using a TE011 and quasi TE0mn Mode Dielectric Resonators," *Cryogenics*, vol. 46, pages 730-735, 2006.

[8] J. Krupka, K. Derzakowski, A. Abramowicz, M. E. Tobar, and R. G. Geyer, "Complex permittivity measurements of extremely low loss dielectric materials using whispering gallery modes," *Proc. IEEE MTT Int. Micr. Sym. Digest*, Denver, vol. 3, pages 1347 - 1350, 1997.

[9] J. Krupka, K. Derzakowski, M. E. Tobar, J. G. Hartnett, and R. G. Geyer, "Complex permittivity of some ultralow loss dielectric crystals at cryogenic temperatures," *Meas. Sci. Technol.*, vol. 10, pages 387-392, 1999.

[10] J. Krupka, K. Derzakowski, A. Abramowicz, M. E. Tobar, and R. Geyer, "Use of whispering gallery modes for complex permittivity determinations of ultra-low-loss dielectric materials," *IEEE Trans. on MTT*, vol. 47, pages 752-759, 1999.

[11] V.B. Braginsky, V.P. Mitrofanov, V.I. Panov, *Systems with small dissipation* (University of Chicago Press, Chicago, 1985).

[12] A.G. Mann and J. Krupka "Measurements of susceptibility due to paramagnetic impurities in sapphire using whispering gallery modes," *Microwaves, Radar and Wireless Communications. MIKON-2000. 13th International Conference on* vol. 2, pages 421-424, 2000

[13] A.E. Siegman, *Microwave Solid-state Masers*, McGraw-Hill Electrical and Electronic Engineering Series, (MacGraw-Hill, New York, San Francisco, Toronto, London, 1964).

[14] A.E. Siegman, *Lasers*, (Oxford University Press, Oxford, 1986).

[15] A.R. Smith, "Anisotropic magnetic susceptibilities of vanadium and titanium ions in corundum," in Report Texas Tech University, 1970

[16] T. Tatsukawa, T. Shiai, T. Imaizumi, T. Idehara, I. Ogawa, and T. Kanemaki, "Ruby ESR over a wide frequency range in the millimeter wave region," *Int. J. Infrared Millimeter Waves*, vol. 19, pages 859-873, 1998.

[17] M. E. Tobar, A.G. Mann, "Resonant frequencies of high order modes in cylindrical anisotropic dielectric resonators," *IEEE Trans on MTT*, vol. 39, pages 2077-2083, 1991

[18] M. E. Tobar, J. Krupka, E. N. Ivanov, and R. A. Woode, "Anisotropic complex permittivity measurements of mono-crystalline rutile between 10-300 K," *J. of Appl. Phys*, vol. 83, pages 1604-1609, 1998.

[19] M.E. Tobar, J.G. Hartnett, "Proposal for a new test of the time independence of the fine structure constant, α , using orthogonally polarised whispering gallery modes in a single sapphire resonator," *Phys. Rev. D*, vol. 67, 062001, 2003.